Satellite and Radar Survey of Mesoscale Convective System Development

ISRAEL L. JIRAK, WILLIAM R. COTTON, AND RAY L. MCANELLY

Colorado State University, Fort Collins, Colorado

(Manuscript received 14 November 2002, in final form 7 April 2003)

ABSTRACT

An investigation of several hundred mesoscale convective systems (MCSs) during the warm seasons (April–August) of 1996–98 is presented. Circular and elongated MCSs on both the large and small scales were classified and analyzed in this study using satellite *and* radar data. The satellite classification scheme used for this study includes two previously defined categories and two new categories: mesoscale convective complexes (MCCs), persistent elongated convective systems (PECSs), meso-β circular convective systems (MβCCSs), and meso-β elongated convective systems (MβECSs). Around two-thirds of the MCSs in the study fell into the larger satellite-defined categories (MCCs and PECSs). These larger systems produced more severe weather, generated much more precipitation, and reached a peak frequency earlier in the convective season than the smaller, meso-β systems. Overall, PECSs were found to be the dominant satellite-defined MCS, as they were the largest, most common, most severe, and most prolific precipitation-producing systems.

In addition, 2-km national composite radar reflectivity data were used to analyze the development of each of the systems. A three-level radar classification scheme describing MCS development is introduced. The classification scheme is based on the following elements: presence of stratiform precipitation, arrangement of convective cells, and interaction of convective clusters. Considerable differences were found among the systems when categorized by these features. Grouping systems by the interaction of their convective clusters revealed that more than 70% of the MCSs evolved from the merger of multiple convective clusters, which resulted in larger systems than those that developed from a single cluster. The most significant difference occurred when classifying systems by their arrangement of convective cells. In particular, if the initial convection were linearly arranged, the mature MCSs were larger, longer-lived, more severe, and more effective at producing precipitation than MCSs that developed from areally arranged convection.

1. Introduction

Mesoscale convective systems (MCSs) are significant rain-producing weather systems for the central United States during the warm season (Fritsch et al. 1986). Additionally, MCSs produce a broad range of severe convective weather events (Maddox et al. 1982; Houze et al. 1990) that are potentially damaging and dangerous to society in general. Given the profound influence that MCSs have on the midlatitudes, continued study is essential in gaining a deeper insight of these systems.

Even though the importance of MCSs is well understood, there is much left to learn about the growth and development of these systems. One approach that has been used to study MCSs involves classifying the systems and analyzing the differences among the categories. For example, infrared satellite imagery has been an important means of studying a particular type of MCS called the mesoscale convective complex (e.g., Maddox 1980, 1983; Maddox et al. 1982; McAnelly and Cotton 1986; Cotton et al. 1989). Although satellite images provide an effective way of identifying MCSs, they do not provide much information on the underlying convection. Consequently, radar data have been used to allow for more detailed classification studies of MCS convection (e.g., Bluestein and Jain 1985; Bluestein et al. 1987; Houze et al. 1990; Parker and Johnson 2000).

While both satellite and radar data have been used independently to study samples of MCSs, there have not been any large, detailed MCS inquiries using *both* types of data. Additionally, previous studies have generally focused on a particular type of MCS, but this study examines circular and elongated systems on both the large and small scales. The purpose of this investigation is to supplement prior studies on MCS classification by providing a more comprehensive satellite and radar survey of MCSs in terms of number of systems, type of systems, length of study, and geographical area considered. The focus of the classification scheme is directed toward the developmental stages to better characterize common patterns by which convection becomes organized into mature MCSs.

Relevant observational MCS studies done in the past are discussed and related to the present study in section

Corresponding author address: Israel L. Jirak, Department of Atmospheric Science, Colorado State University, Fort Collins, CO 80523.
E-mail: ijirak@atmos.colostate.edu

TABLE 1. Modified mesoscale convective complex (MCC) definition.

	Physical characteristics
Size	Cloud shield with continuously low IR temperature ≤ -52°C must have an area $\geq 50\,000$ km^2.
Initiate	Size definition is first satisfied.
Duration	Size definition must be met for a period ≥ 6 h.
Maximum extent	Contiguous cold cloud shield (IR temperature ≤ -52°C) reaches a maximum size.
Shape	Eccentricity (minor axis/major axis) ≥ 0.7 at time of maximum extent.
Terminate	Size definition no longer satisfied.

2. Section 3 provides an overview of the data and methods used in this analysis. The infrared satellite classifications are defined and discussed in section 4 with some basic comparisons. Section 5 discusses the method used to categorize the development of MCSs as seen by radar imagery. In addition, this section provides some examples and basic characteristics of each category. Further analysis of the environment, severe weather, and life cycles of each MCS category is provided in section 6. Finally, section 7 provides a summary and conclusions.

2. Background

Several MCS studies performed in the past have attempted to classify MCSs into discrete categories by a variety of different methods and perspectives. The most common methods of MCS classification have involved analyzing satellite and radar characteristics of the systems. Similar to past studies, the present study attempts to classify MCSs to better understand the similarities and differences between the systems; however, unlike past studies, this study will classify each MCS by *both* satellite and radar characteristics. Several studies on the classification of MCSs by satellite and radar characteristics have emerged in the past 20 yr, and the most influential studies are discussed in the following subsections.

a. Satellite classification of MCSs

Maddox (1980) first classified a particular type of MCS by means of satellite imagery. He noticed a high frequency of organized, quasi-circular, meso-α (see Orlanski 1975) convective weather systems moving across the central United States. He termed these massive systems *mesoscale convective complexes* (*MCCs*). He based the definition of MCCs on typical infrared satellite characteristics possessed by systems moving across the central United States. The only minor modification that has been made to Maddox's original definition of MCCs was by Augustine and Howard (1988) to remove the ≤ -32°C size requirement of the cloud shield in order to simplify the identification and documentation procedure of MCCs. This modified MCC definition is shown in Table 1 and is used in the current study. It is noteworthy to mention that Cotton et al. (1989) set forth an alternative dynamical definition of MCCs, which relates the horizontal scale of MCCs to the Rossby radius of deformation. Another large class of MCSs, persistent elongated convective systems (PECS), was identified in a study by Anderson and Arritt (1998). PECS are what might be considered the ''linear'' version of MCCs, as the only difference between a MCC and a PECS is the shape of the system (Table 2). PECSs have eccentricities between 0.2 and 0.7 while MCCs must have eccentricities ≥ 0.7. The definitions of MCCs and PECSs will be used along with two other definitions to include smaller MCSs in a satellite classification scheme for this study.

b. Radar classification of MCSs

Unlike the relatively objective satellite classification process, the radar classification process is much more subjective. Two basic methods of categorizing MCSs by radar characteristics have evolved over time. One common method has been to examine the arrangement of the convective and stratiform regions of a mature MCS, including classifications such as leading-line/trailing stratiform (TS), parallel stratiform (PS), and leading stratiform (LS) MCSs (e.g., Houze et al. 1990; Parker and Johnson 2000). Another common, yet different, method of MCS radar classification has been to classify MCSs based on their developmental or for-

TABLE 2. MCS definitions based upon analysis of IR satellite data.

MCS category	Size	Duration	Shape
MCC	Cold cloud region ≤ -52°C with area $\geq 50\,000$ km^2	Size definition met for ≥ 6 h	Eccentricity ≥ 0.7 at time of maximum extent
PECS			$0.2 \leq$ Eccentricity < 0.7 at time of maximum extent
MβCCS	Cold cloud region ≤ -52°C with area $\geq 30\,000$ km^2 and maximum size must be $\geq 50\,000$ km^2	Size definition met for ≥ 3 h	Eccentricity ≥ 0.7 at time of maximum extent
MβECS			$0.2 \leq$ Eccentricity < 0.7 at time of maximum extent

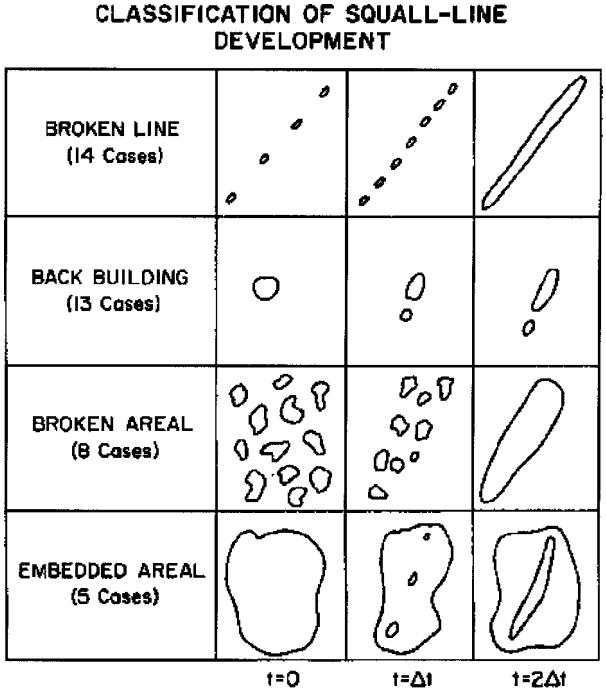

FIG. 1. Idealized depictions of squall-line formation (from Bluestein and Jain 1985).

mative stages (e.g., Bluestein and Jain 1985; Bluestein et al. 1987; Blanchard 1990; Loehrer and Johnson 1995). As previously mentioned, the focus of this study lies in the development of MCSs, so only those studies relating to this topic will be discussed further.

Bluestein and Jain (1985) performed the first study of this type seeking to identify common patterns of severe squall-line formation. They considered the general definition of squall line (i.e., ''a linearly oriented mesoscale convective system'') in their examination of data from a single-radar site over central Oklahoma. Squall-line development was divided into four classifications: broken line, back building, broken areal, and embedded areal (see Fig. 1). The broken-line and back-building categories were the most common type of formation and were the easiest to distinguish using satellite imagery. However, they made no attempt beyond this to observe and classify squall lines by satellite characteristics. In a closely related study, Bluestein et al. (1987) studied the formation of nonsevere squall lines in Oklahoma and found that the broken-areal category was the most common type of formation for nonsevere squall lines.

Other studies on the classification of MCS development also provided some framework for the current study. Blanchard (1990) identified three mesoscale convective patterns for the Oklahoma–Kansas Preliminary Regional Experiment for STORM-central (PRESTORM) field program: linear convective systems, occluding convective systems, and chaotic convective systems (see Fig. 2). In relation to the present study, the most important feature of this study is the inclusion of all types of MCSs (i.e., both linear and nonlinear) in the classification scheme. Another more recent study by Loehrer and Johnson (1995) looked at different developmental paths of MCSs to reach an asymmetric TS structure. Disorganized, linear, back-building, and intersecting convective bands were the four modes of development they identified (see Fig. 3). An important aspect of their classification is the idea of including the interaction between convective bands as a mode of development. With these previous studies serving as a foundation, the current survey provides further insight on MCS development.

3. Data and methods of analysis

The advancement and availability of digitized data and computing power have allowed studies to become increasingly comprehensive with time. One goal of this study was to sample a large number of MCSs; thus, a reasonably long time period and large domain were selected to reach that goal. Based on MCS studies mentioned previously, the range of April through August seemed to be an appropriate time frame to study the active convective season of the central United States. Furthermore, a 3-yr period was selected to obtain a large and varied sample of MCSs with a minimal annual bias. Any MCS that had its convective initiation between 24°–51°N and 82°–115°W was considered for this study as large, organized convective weather systems occur frequently in this area. This large spatial domain covers the central United States and excludes only areas west of the Rocky Mountains and east of the Appalachian Mountains in the United States.

a. Satellite data

Infrared satellite imagery was used to initially identify the sample of MCSs. Generally speaking, it is easier to identify MCSs by their cold cloud shield than by their radar reflectivity patterns, as the underlying convection can take many forms. In addition, the cold cloud shield is larger than the area of convection and often is more contiguous, making it easier to identify and study a large number of systems. The satellite data for the 3-yr period (1996–98) were obtained from the Global Hydrology Resource Center (GHRC) at the Global Hydrology and Climate Center in Huntsville, Alabama. The dataset is comprised of hourly global composite infrared images at 14-km resolution in the horizontal. Occasionally, there were missing data (most notably 1–7 July 1996), but overall it was a consistent dataset that provided fundamental information about each MCS. The hourly satellite images were reviewed, and any system developing in the region of interest that appeared to have persistent, coherent structure at the $-52°C$ temperature threshold was recorded as a MCS. This subjective first stage of identification resulted in an initial sample of 643 MCSs

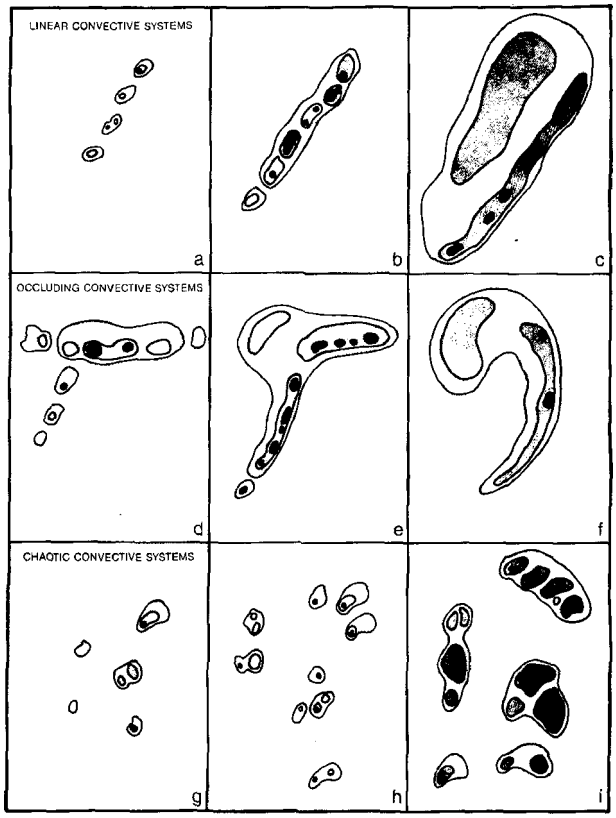

FIG. 2. Schematic reflectivity evolution of three convective modes during the PRE-STORM program: (a), (b), (c) linear convective systems; (d), (e), (f) occluding convective systems; and (g), (h), (i) chaotic convective systems (from Blanchard 1990).

of all shapes and sizes. Next, a modified version of a MCC documentation program written by Augustine (1985) was used to gather hourly size, centroid, and eccentricity information for each MCS over its lifetime. Several more systems were discarded during this step due to a lack of system cohesiveness, missing data, or domain issues. Consequently, a total of 514 systems were left for the satellite classification process, which will be discussed in section 4.

b. Radar data

While satellite imagery is useful for getting a broad viewpoint of MCSs, it lacks detail for studying the smaller-scale internal precipitation structure of MCS development. Therefore, radar reflectivity data were used to examine the systems at a higher temporal and spatial resolution. Since the MCSs had already been identified by means of infrared satellite, the radar data could be used to study the development and arrangement of the underlying convection of these predetermined systems. The radar images, which were also obtained from the GHRC, are national reflectivity composites providing very convenient images for examining a significant portion of the United States. The data are arranged into 16 intensity bins at 5-dBZ increments with a horizontal resolution of 2 km $\times$ 2 km and are available at 15-min intervals. Since the dataset was easy to work with and had very little missing data, it proved to be a useful tool for viewing the development of MCSs over the central United States. The first stage of radar analysis involved reviewing the radar images and associating the radar echoes with the cloud shields of the MCSs. Many of the systems did not have sufficient radar coverage to analyze the developmental stages. This was certainly expected as the geographical region considered extends beyond the radar coverage of the continental United States. Consequently, there was a total of 387 MCSs with a complete set of both satellite and radar data. Next, another modified version of Augustine's (1985) program was developed to work with the radar data to obtain size, centroid, eccentricity, and reflectivity characteristics for the radar life cycle of each MCS. The Z–R relationship used to calculate the rain rate in this study was proposed by Woodley et al. (1975):

$$Z = 300R^{1.4}.$$

This relationship is used by the GHRC when producing composite daily rainfall maps and is also the default algorithm used for the Weather Surveillance Radar-1988 Doppler (WSR-88D) radars (Fulton et al. 1998). Even though the radar images are quality controlled, it is worth mentioning that there still may be instances of radar attenuation, brightband effects, and anomalous propagation that may alter the actual reflectivity fields. Nevertheless, when extracting quantitative measurements, an attempt was made to minimize these effects by only looking at the averages of a large number of systems. Finally, the development of each system was analyzed by animating the 15-min radar images. This process and the resulting classification scheme will be discussed in much more detail in section 5.

c. Sounding data and severe weather reports

Sounding data were also used in analyzing the MCS sample to provide some information on the environment in which the MCSs formed. The National Weather Service sounding data were obtained from an online archive maintained by the University of Wyoming Department of Atmospheric Science. Similar to previous MCS studies (e.g., Houze et al. 1990; Parker and Johnson 2000), an individual sounding was chosen to be the most representative sounding of the air mass in which the MCS formed and was used without modification. Further efforts to interpolate nearby soundings (see Bluestein and Parks 1983; Bluestein and Jain 1985) or to modify operational soundings with numerical models (see Brooks et al. 1994) were not undertaken due to the large volume of MCSs studied and to focus on information available to the operational forecaster. Sounding properties were computed for each individual sounding, grouped into

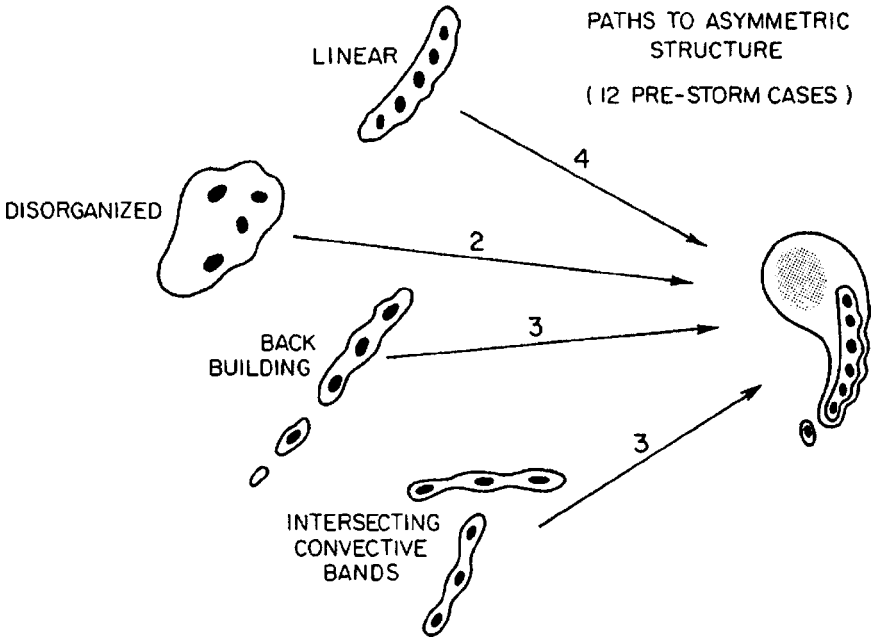

FIG. 3. Schematic of the paths to reach asymmetric structure observed by Loehrer and Johnson (1995; from Hilgendorf and Johnson 1998).

the appropriate MCS classification, and averaged for each category.

In addition, severe weather reports were obtained from an online archive maintained by the National Oceanic and Atmospheric Administration (NOAA) Storm Prediction Center (SPC). An interactive program developed by the SPC, *SeverePlot*, allowed for the straightforward tabulation of severe-weather reports for a selected area and time period. As a result, the number of tornado, wind, and hail reports was recorded for the entire life cycle of each MCS along with any reported injuries or deaths. A discussion of the results is provided in section 6.

4. Satellite classification of MCSs

We have seen that the classification of MCSs by satellite characteristics has been done in the past; however, there has been little recognition of *all* types of MCSs (i.e., circular and elongated systems on both the large and small scales) in the same study using satellite imagery. The satellite classification scheme presented in this section attempts to build upon previous studies by being more inclusive of MCSs, especially smaller systems. The satellite classification scheme and basic characteristics of each category are presented in the following sections.

a. Definition of classes

The cornerstone of MCS classification by satellite imagery is the definition of MCCs by Maddox (1980). Thus, the method he used to define MCCs along with modifications made by Augustine and Howard (1988) formed the basis of the classification scheme used in this study. Essentially, the systems were classified according to their size, duration, and eccentricity of the $-52°C$ cloud-top temperature threshold. As discussed in section 2, large MCSs, MCCs, and PECSs, have been well defined and documented. Consequently, these systems comprise two of the four satellite-defined categories. The relatively undocumented systems are the smaller MCSs; therefore, categories are defined to include these systems.

Since the large MCSs are discriminated by shape (i.e., MCC for circular systems and PECS for linear systems), it is natural to create two categories for smaller MCSs: one for circular systems and one for linear systems. Consequently, the eccentricity criterion for the smaller systems will be the same as for the larger systems. The only criteria left to be defined for the smaller systems are the size and duration of the cloud shield at the $-52°C$ threshold. These minimum criteria are important because they basically set the definition of a MCS for this study. As discussed in Parker and Johnson (2000), the appropriate MCS timescale is f^{-1}, which is approximately 3 h for the midlatitudes. Thus, the duration criterion for the smaller MCSs is set at ≥ 3 h.

The size criterion is somewhat more difficult and arbitrary to assign for the smaller systems than the timescale. Some studies have suggested an MCS length scale of 100 km (e.g., Houze 1993; Geerts 1998; Parker and Johnson 2000). This seems appropriate, but they were

considering the scale of convective radar echoes, and cloud shields grow much larger than the area of the underlying convection. Systems with radar echoes of 100 km or more in length seemed to generally have cloud shields of at least 30 000 km^2 in area (approximately the area of a circle with a radius of 100 km). The reexamination of the small systems also led to the conclusion that the most coherent systems maintained an area of at least 30 000 km^2. Thus, the size criterion for the smaller systems was set at $\geq$30 000 km^2 with the caveat that their maximum size must be at least 50 000 km^2 as a way of connecting the definition of the smaller systems to the larger systems. To keep the naming convention as simple as possible, the smaller circular systems are referred to as *meso-β circular convective systems* (MβCCSs) and the smaller linear systems are called *meso-β elongated convective systems* (MβECSs). From Orlanski's (1975) definitions of meteorological scales, the larger and longer-lasting MCSs fit more appropriately into the meso-α scale while the smaller and shorter-lived MCSs fit more appropriately into the meso-β scale; hence, the reasoning for the nomenclature. Table 2 shows the definitions of the four classes of MCSs according to infrared satellite characteristics: MCC, PECS, MβCCS, and MβECS. The terminology used to denote different MCS life cycle stages is the same as defined by Maddox (1980): *initiation* is the time when the MCS size definition is first met, *maximum extent* is the time when the cold cloud shield reaches a maximum size, and *termination* occurs when the MCS no longer satisfies its size definition.

b. Basic characteristics

As discussed in section 3, 514 systems were identified and subjected to the satellite classification scheme. During the classification process, 49 systems were removed from consideration for not meeting the definition of one of the satellite categories, which left 465 classifiable MCSs.

Figure 4 provides a breakdown of MCS frequency for each of the 5 months during the 3-yr period. Examination of the figure reveals that in every month more systems fit into the larger MCS classifications (MCCs and PECSs) than the smaller MCS classifications (MβCCSs and MβECSs). The nature of the MCS definitions used in this study allows the inclusion of only the most coherent, persistent systems; thus, a lower size limit was used without an analogous upper size limit to retain just the significant MCSs. As a result, more systems in this study fall into the larger MCS classifications even though smaller systems are actually more common as seen in Fig. 5. This figure supports the general expectation of an exponential decrease in the number of MCSs when moving toward larger systems (Cotton et al. 1995). Figure 4 shows that MCCs and PECSs accounted for 64% of the MCSs during the study period; PECSs were the most common type of MCS, accounting

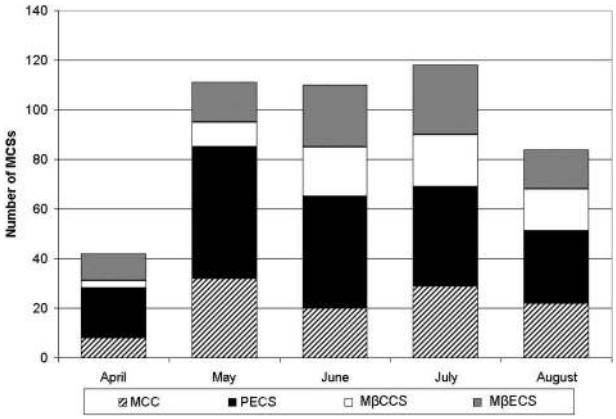

FIG. 4. Distribution of all MCSs by month.

for 40% of the sample total. As far as the monthly totals are concerned, May, June, and July had about equal chances for MCS occurrence. April was by far the least-likely month for a MCS to develop, accounting for less than 10% of the sample total. Another observation is that the greatest frequency of smaller systems tended to occur later in the season (July) as opposed to the larger systems, which had a peak frequency in May.

Average statistics for each MCS class can be found in Table 3. PECSs had the largest average maximum area of over 200 000 km^2 while the smaller systems had average maximum areas under 100 000 km^2. The larger systems persisted longer on average (10 h) than the smaller systems (6 h), as would be expected due to the nature of the duration criteria in their definitions. The shape did not appear to have much influence on the duration of the system, as MCCs and PECSs had nearly identical average durations, and MβCCSs and MβECSs also had very similar durations. The average lifetime of all MCSs was over 9 h. The average and standard deviation of the eccentricities for each type of MCS are also listed in Table 3. The circular systems, MCCs and MβCCSs, had very similar eccentricities, and the linear systems, PECSs and MβECSs, also had very similar eccentricities with average values in the middle of their respective ranges.

The distribution of times at which these systems reached initiation, maximum extent, and termination can be found in Fig. 6. The frequency of times of MCS initiation is displayed at the front of the graph. Nearly 60% of all MCSs were initiated between 2000 and 0300 UTC, which corresponds to the afternoon and evening hours of the central United States. Figure 6 also shows the distribution of times of maximum extent for all MCSs. About 60% of the systems reached their maximum size between 0200 and 0900 UTC, or about 6 h after initiation. Finally, the last set of data at the back of Fig. 6 shows the distribution of times of termination for the MCS sample. Most of the systems dissipated between 0700 and 1500 UTC, or during the morning

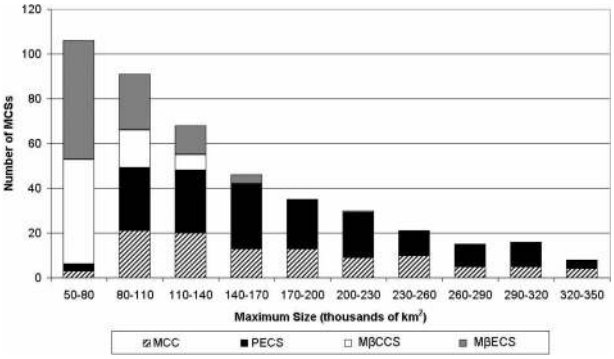

FIG. 5. Distribution of all MCSs as a function of size.

hours of the central United States. Thus, as was found in Maddox's (1980) MCC study and other MCS studies, a majority of the systems in this study formed in the late afternoon and evening hours, reached their maximum size during the night, and dissipated in the early morning hours.

5. Radar classification of MCSs

Similar to classifying MCSs by satellite characteristics, there have been many studies classifying MCSs by radar characteristics. Unfortunately, the radar studies have not necessarily been well connected with one another or with the satellite classification studies. In addition, convective lines were often the only types of MCSs considered in the radar studies. The radar classification scheme presented in this study examines the development of a wide variety of MCSs.

An effort was made to be consistent with previous studies using similar terminology wherever possible to avoid confusion. The foundation of the classification scheme presented in this section was provided by Bluestein and Jain's (1985) study on the formation of severe squall lines. However, since they only considered squall lines, the scheme needed to be expanded to accommodate all types of MCSs. The goal was to try to characterize the interaction of the convective cells and clusters underneath the cloud shield.

a. Definition of classes

Bluestein and Jain (1985) used four classes to describe squall-line development: broken line, back building, broken areal, and embedded areal (see Fig. 1). Following their study, the terms *embedded*, *areal*, and *line* were implemented into the current scheme. Some important factors considered in creating the scheme included the orientation, number, and interaction of convective cells and clusters as well as the presence of stratiform precipitation. Consideration of these factors led to a classification scheme of three levels. First, the systems were categorized based on whether or not stratiform precipitation existed in the area where convection was initiated. Second, the systems were sorted by the arrangement of the initial cellular convection. Last, the systems were classified by the number of convective clusters and how they interacted. The following sections provide more detail on each level of this classification scheme.

TABLE 3. Statistics for each MCS satellite classification: Means and std devs ( ).

	No.	Maximum area (km²)	Duration (h)	Eccentricity
MCC	111	193 282 (108 146)	10.9 (3.9)	0.83 (0.09)
PECS	187	213 473 (130 020)	10.6 (3.8)	0.50 (0.13)
MβCCS	71	74 696 (21 540)	6.1 (2.2)	0.84 (0.08)
MβECS	96	85 195 (29 786)	6.7 (2.1)	0.53 (0.11)
All MCSs	465	160 980 (116 140)	9.2 (3.9)	0.64 (0.19)

1) PRESENCE OF STRATIFORM PRECIPITATION

The first level in the classification scheme involved determining whether or not the initial convection formed in an area of stratiform precipitation. This step follows directly from Bluestein and Jain's (1985) embedded areal systems, which were found to develop in areas of significantly lower CAPE than the other types of squall-line development. Thus, due to such anticipated differences between embedded systems and those that formed in nonprecipitating areas, a level of the classification process was devoted to identifying the presence of stratiform precipitation. This step was generally straightforward because the systems usually either formed in echofree regions or in areas with significant stratiform precipitation. As seen in Fig. 7, if any convective cluster were initiated in a region of stratiform precipitation, the system was tagged with the term *embedded*. If a system did not form in a region of stratiform precipitation (i.e.,

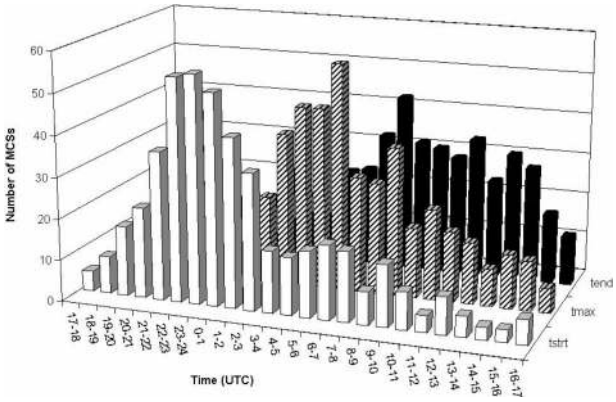

FIG. 6. Distribution of all MCSs as a function of initiation time (tstrt), time of maximum extent (tmax), and termination time (tend).

not embedded), it was not given a label for this level of the classification scheme.

2) ARRANGEMENT OF CONVECTIVE CELLS

The next level in the classification scheme described the arrangement of convective cells at initiation. Once again, this follows closely from Bluestein and Jain (1985) who categorized cellular arrangement into line and areal categories. Thus, this step involved analyzing the early stages of convection to determine whether or not the cells were arranged in a line. Figure 7 shows that systems with convection organized in a linear fashion received the term *line* while systems with scattered convection (i.e., not arranged linearly) received the term *areal.* If a system were comprised of convective clusters with both types of cellular arrangement, it was given the term *combination.* Keep in mind that this step does not necessarily provide information on the shape of the MCS at its maturity. As Bluestein and Jain (1985) showed, areal systems can develop into squall lines.

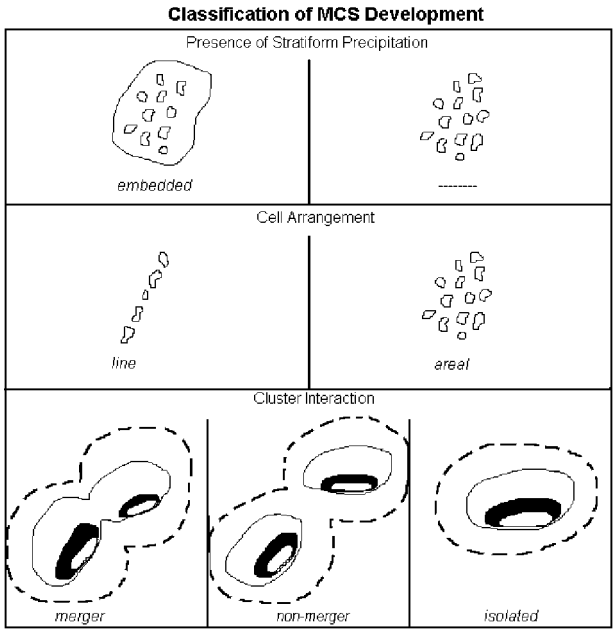

FIG. 7. Idealized depiction of the three-level classification scheme used to categorize MCS development as seen by radar. The solid lines and contours represent relative reflectivity levels while the dashed lines represent the outline of the cold cloud shield.

3) INTERACTION OF CONVECTIVE CLUSTERS

The final level in the classification scheme involved observing how the convective cells grew into clusters and interacted with other convective clusters. This necessarily involved stages later into the life cycle of the MCSs (generally to about the time of maximum extent) and was the most subjective step in the classification scheme. The term *cluster* referred to a meso-β grouping of convective cells that were contiguous or nearly contiguous. Independent convective clusters were distinguished from one another by physical separation between convection, difference in orientation from surrounding convection, and initiation of convection at different times. Three major features of cluster interaction emerged, and the systems were categorized accordingly. One type of interaction involved the growth of convective cells into a single convective cluster. These systems were termed *isolated* systems (see Fig. 7). Another type of interaction involved the development of multiple independent convective clusters that merged into a single entity. These systems were given the name *merger* systems. Finally, if individual convective clusters developed close enough to one another to share a common cloud shield, but did not physically merge as seen by radar, then they were termed *nonmerger* systems. The nonmerger systems appear the same as merger systems when viewed by satellite imagery; however, examination of radar imagery reveals that they are very different in the fact that the underlying convective clusters do not merge together. Consequently, both satellite and radar data must be examined to classify these systems, which is a feature unique to this study that was not a part of previous MCS studies.

The nature of the classification scheme as seen in Fig. 8 leads to 17 categories, including an unclassifiable category and four combination categories. The unclassifiable category contains systems that could not be classified in one or more of the levels of classification scheme. The combination categories arise from systems with clusters that develop from a mixture of line and areal arrangements. Also, note that isolated systems cannot have a combination category since they develop from a single convective cluster. Of course, not all categories are guaranteed to include many systems since this was a classification *process,* rather than just a list of the most important categories.

To illustrate the flexibility and usefulness of this new scheme, it will be used to classify the various categories from previous MCS development studies. From Bluestein and Jain's (1985) study (Fig. 1): the broken-line category would be classified as a line isolated system, the back-building category would also be classified as a line isolated system, the broken areal category would be classified as an areal isolated system, and the embedded areal category would be classified as an embedded areal isolated system. From Blanchard's (1990) study (Fig. 2): the linear convective system would be classified as a line isolated system, the occluding convective system would be classified as a line merger, and the chaotic convective system (as represented in the figure without widespread stratiform precipitation) would be classified as an areal nonmerger. From Loehrer and Johnson (1995) (Fig. 3): the linear system would be classified as a line isolated system, the disorganized system would be classified as an areal isolated system,

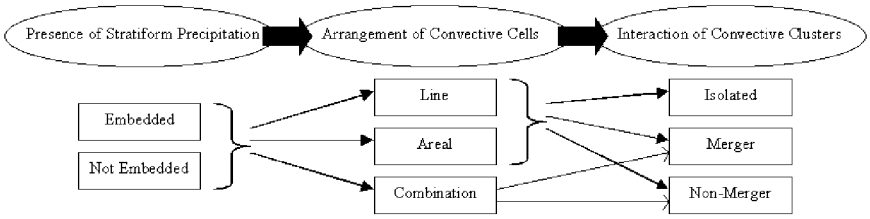

FIG. 8. Flow chart describing the radar classification scheme, which consists of 16 categories plus an unclassifiable category.

the back-building category would be classified as a line isolated system, and the intersecting convective bands would be classified as a line merger.

b. Examples of classes

In order to show what the development of some of these systems looks like, this section provides radar imagery for examples of the six most common types of MCS development. Four images at various times throughout each type's life cycle are supplied to provide an idea of how the MCSs were classified by their development. Areal mergers were the most frequent type of MCS development in this study. A typical areal merger system occurred on 20 June 1996, as shown in Fig. 9. The panels show initial scattered convection in southern Arkansas and northern Louisiana that developed into three distinct convective clusters and ultimately merged into a mature MβCCS by 0900 UTC moving to the southwest. Closely related to the areal merger system is the combination merger system, which was the second most common type of MCS development found in this study. The only difference between these types of development is that some of the initial convection in a combination merger system is arranged in a line. Figure 10 shows an example of such a system that occurred on 24–25 June 1997. The initial convection in southeastern Colorado was of the areal variety while the convection extending from southern Nebraska to western Iowa was of the linear variety, thus, making it a combination system. These distinct convective clusters merged several hours later into a mature PECS.

The next most common type of system was an areal isolated system, which evolves from a single convective cluster that forms from scattered convection. An example of this type of system developed in northern Texas on 4–5 June 1996 as seen in Fig. 11. Two distinct convective clusters emerged by 0100 UTC, but the northern cluster (located along the northern fringe of the cloud shield) dissipated rapidly several hours before the system reached maturity, thus, having little effect on MCS development. The southern cluster grew into a MCC by 0800 UTC as it moved to the southeast. Figure 12 shows a representative line merger system that occurred on 21–22 June 1997 in the upper Midwest. Linearly arranged convection developed into several distinct convective clusters and merged into a PECS with a well-defined TS arrangement. The next example is an embedded areal merger that occurred in South Dakota on 25 August 1997. As seen in Fig. 13, the initial convection developed in a general area of stratiform precipitation; thus, the system was termed as embedded. Later, distinct convective clusters merged to form a mature MβCCS. Notice that the cloud shield of this system did not encircle the radar reflectivity echoes as well as the previous examples, which was a common feature of the embedded systems. The final example of MCS development is an areal nonmerger system that occurred along an axis east of the Rocky Mountains on 26–27 May 1998. Figure 14 shows that scattered convection throughout Wyoming and Colorado developed into individual convective clusters. Interaction occurred between these areal clusters as their cloud shields merged to form a PECS; however, the convection itself did not merge, resulting in its classification as a nonmerger system. It should be noted that this was a relatively extreme example of a nonmerger system and was used to clearly illustrate the nonmerging precipitation shields under a common cloud shield.

c. Basic characteristics

As was discussed in section 3, a total of 387 systems remained after the final stages of radar analysis and screening. The radar images were animated and observed for the life cycle of each system to scrutinize, analyze, and ultimately categorize the development of each system. It is important to keep in mind that the statistical results presented here and throughout the remainder of the paper are strongly influenced by the scheme developed to categorize MCSs. Even though this classification scheme is subjective, it will hopefully prove to be flexible and functional for future MCS studies.

Table 4 lists the distribution of MCS development according to each system's satellite classification. Note the totals for each development category. The *areal merger* and *combination merger* development categories each accounted for about a quarter of the MCSs. Clearly, the MCSs in this study had a propensity to form by a merger of convective clusters. The next most common types of development were *areal isolated* and *line*

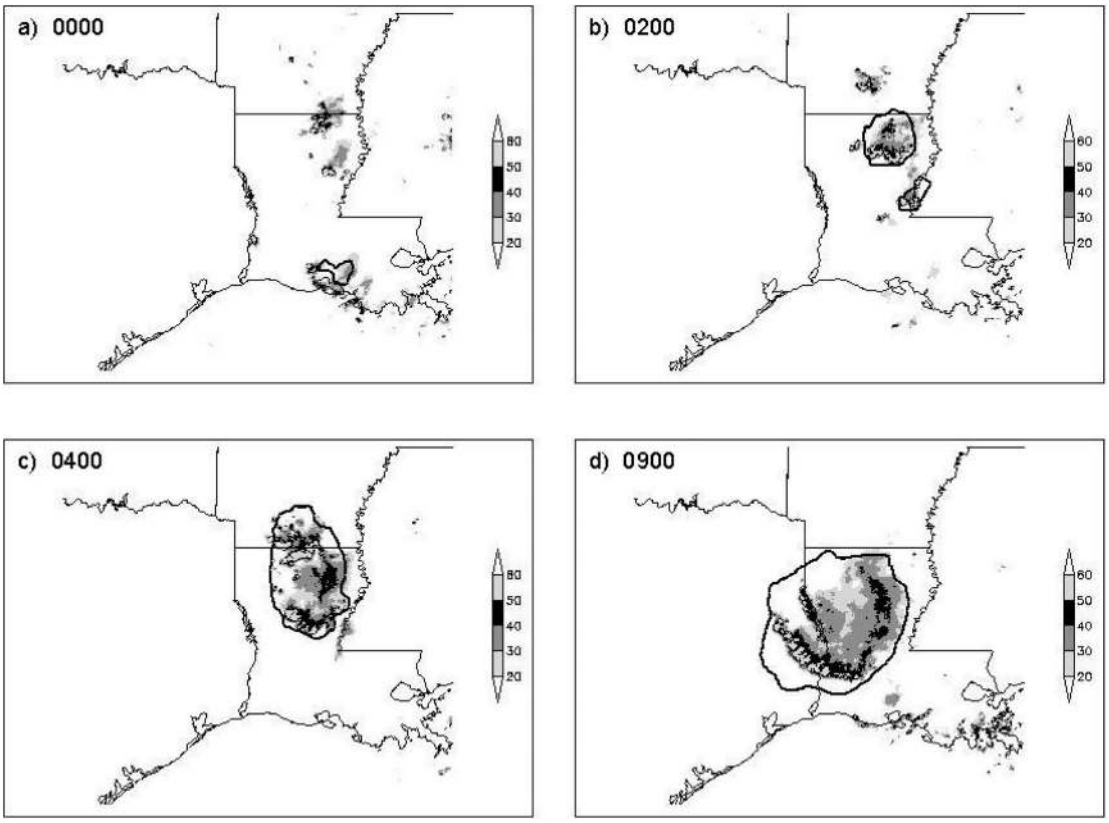

FIG. 9. Areal merger development of a MβCCS that occurred in southern Arkansas and northern Louisiana on 20 Jun 1996, as seen by radar imagery. The radar reflectivity images are from: (a) 0000, (b) 0200, (c) 0400, and (d) 0900 UTC. The solid black contours represent the outline of the −52°C cloud shield.

merger categories. However, each of these categories only accounted for less than 10% of the total MCS sample. Also, it is obvious that the embedded nonmerger systems were not significant types of development in this sample.

Another method that makes it easier to view the results is to break the data into the three levels of the classification scheme. Table 5 presents the data in this fashion. First, note that embedded systems accounted for only 17% of the total MCS sample. A higher percentage (21%) of the smaller satellite-defined systems (MβCCSs and MβECSs) were embedded, compared to the larger systems (14% of MCCs and PECSs). The middle section of Table 5 shows that more than half of the systems had initial convection arranged in an areal fashion. Not too surprisingly, the systems with elongated cloud shields at their maximum extent (PECS and MβECSs) were more likely to have linearly arranged convection at initiation than the circular systems (MCCs and MβCCSs). Finally, merger systems were by far the most common type of cluster interaction accounting for the development of over 70% of the MCSs. Although the nonmerger systems are a distinct class of MCS development, they only occurred about 8% of the time. The data also show that single-cluster, or isolated, systems accounted for a higher frequency of development into smaller systems (MβCCSs and MβECSs). About one-fourth of the meso-β systems were isolated systems while only 15% of the larger systems consisted of a single convective cluster.

A couple of features appear when examining the distribution of MCS development by month. Inspection of the presence of stratiform precipitation reveals that 13 of the 36 MCSs in April, or 36%, were embedded, as compared to only 15% of the total number of systems throughout the remainder of the convective season (i.e., 52 out of 351). The month of April also stands out when considering the arrangement of convective cells. Due to the strong baroclinic forcing early in the season, one-third of all April MCSs (12 out of 36) developed in a linear fashion while only 15% of the systems fell into the line category throughout the rest of the convective season.

The satellite life cycle statistics for each level of radar development are provided in Table 6. Confidence levels were calculated using the Student's *t* test to show statistically significant differences among the properties of various MCS categories. MCSs that were initiated in stratiform precipitation developed into smaller systems at maturity than MCSs that developed in clear air at the

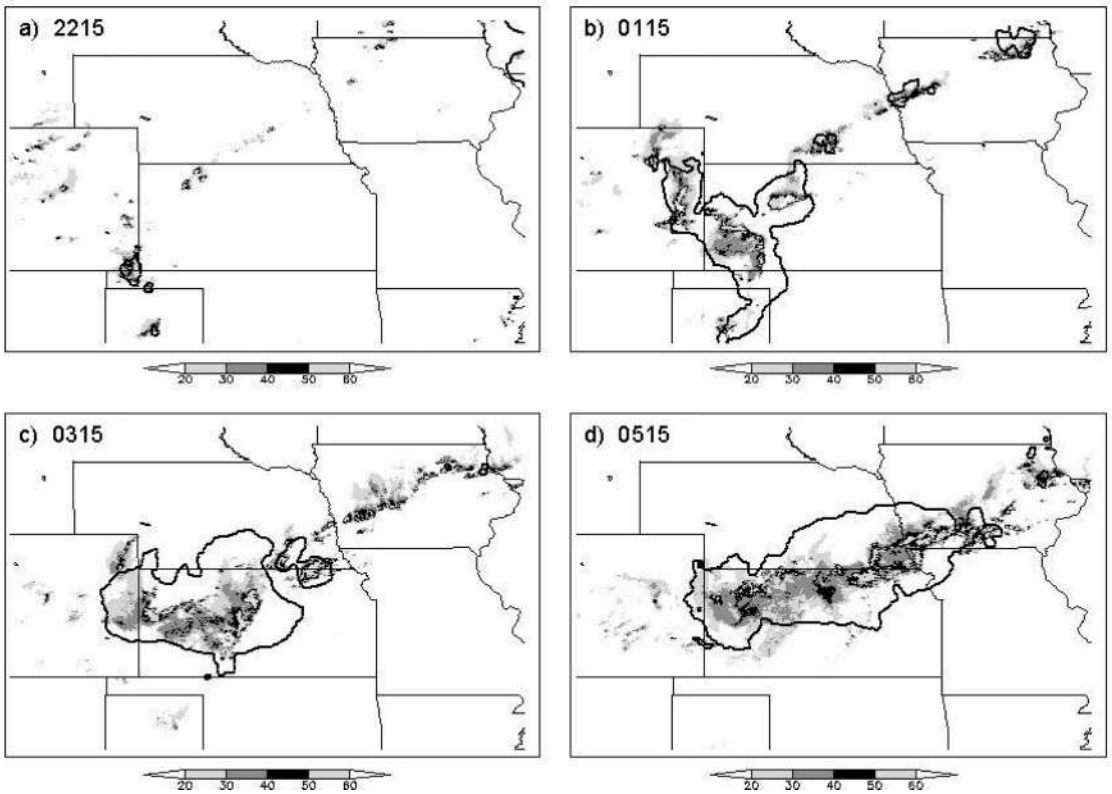

FIG. 10. Combination merger development of a PECS that occurred across CO, KS, and NE, on 24–25 Jun 1997, as seen by radar imagery. The radar reflectivity images are from: (a) 2215 UTC 24 Jun 1997, (b) 0115 UTC, (c) 0315 UTC, and (d) 0515 UTC 25 Jun 1997. The solid black contours represent the outline of the −52°C cloud shield.

99% confidence level. When looking at the statistics for the different types of cell arrangement, the areal systems were smaller and shorter-lived on average than both line and combination systems at the 99% confidence level. This suggests that knowing the arrangement of the initial convection may provide relative information about the duration and maximum size that a system will attain. Also, not surprisingly, systems that had initial convection arranged in a line were more likely to develop a linearly shaped cloud shield as seen by the smaller average eccentricity. The interaction among convective clusters also provides some information on the size of MCSs. If a MCS evolved from a single convective cluster (i.e., isolated system), it was likely to be smaller than a multiple-cluster system (i.e., merger or nonmerger system) at the 99% confidence level. Similarly, McAnelly and Cotton (1986) noted that smaller MCCs tended to develop from a single meso-β convective cluster.

6. Analyses of MCS environment, severe weather, and life cycles

Further analyses of the MCS sample were performed to explore other differences among the various categories. In an effort to learn something about the environmental differences among the MCSs, soundings were selected and examined for each system. Similarly, severe weather reports were logged for each system to study the relationship between severe weather and the various MCS categories. Finally, the satellite and radar life cycles of each MCS classification were composited to investigate possible differences among the systems.

a. MCS environment

The average properties of the soundings for the various MCS classifications were calculated to identify any obvious differences among the environments in which the systems formed. Figure 15 shows a box plot of some common environmental parameters for the various satellite classifications. Parcel properties used in these calculations are based on the mean conditions in the lowest 500 m of the atmosphere. The average values of the severe weather parameters [e.g., CAPE, SWEAT, LI, and BRN (see appendix)] indicate a moderate potential for thunderstorms (Air Weather Service 1979). By reviewing the data in Fig. 15, MβECSs formed in slightly different environments than the other types of MCSs. These systems tended to occur in more stable environments, shown by a lower CAPE and higher LI, than the

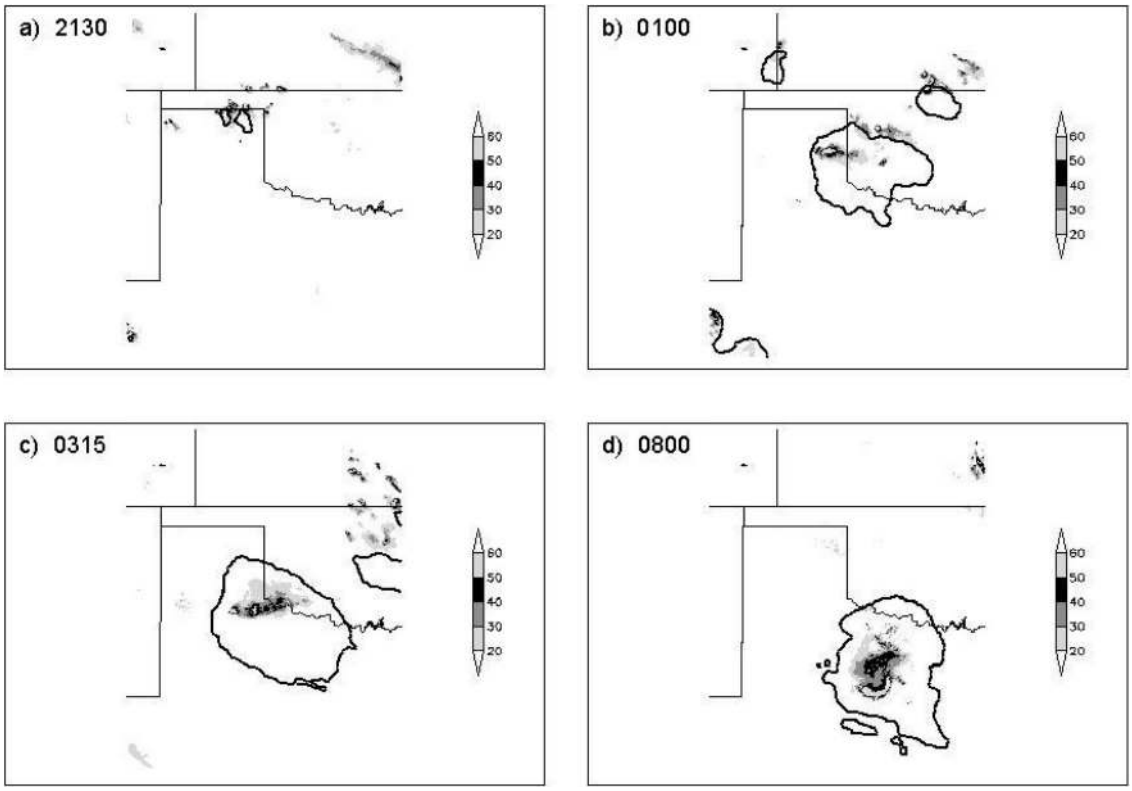

FIG. 11. Areal isolated development of a MCC that occurred in northern TX on 4–5 Jun 1996, as seen by radar imagery. The radar reflectivity images are from: (a) 2130 UTC 4 Jun 1996, (b) 0100 UTC, (c) 0315 UTC, and (d) 0800 UTC 5 Jun 1996. The solid black contours represent the outline of the −52°C cloud shield.

other satellite categories. The SWEAT index shows a statistical difference between the larger MCSs (MCCs and PECSs) and the smaller systems (MβCCS and MβECS). At the 95% confidence level, the smaller MCSs had a lower average SWEAT index than the larger systems. This indicates that the SWEAT index, which was created to help forecast tornadic thunderstorms by including wind shear in its formulation (see appendix), may provide some information about the maximum size of a MCS. Forty-three percent of the larger systems had a SWEAT index greater than 350 while only one-fourth of the smaller systems had a SWEAT index of 350 or greater. A more in-depth analysis of the individual terms of the SWEAT index revealed that MβCCSs and MβECSs had lower SWEAT indices than the larger systems for different reasons. MβCCSs had a lower average SWEAT index because each of the five terms were slightly lower while the MβECSs had a lower average SWEAT index because the Total Totals and 850-mb dewpoint terms were much lower than those of the larger systems.

In a similar manner, Fig. 16 contains average sounding properties for each radar classification of MCS development. This figure reveals a significant difference between the environments of embedded systems and those that do not form in areas of stratiform precipitation. As expected, the environments of embedded systems were much more stable as shown by a lower CAPE and higher LI at greater than the 99% confidence level. The sounding average differences, however, were much less pronounced when dividing the systems according to their cell arrangement and cluster interaction. Areal systems did have a statistically lower average SWEAT index than line and combination systems at the 95% confidence level. An examination of the individual terms of the SWEAT index indicates that the areal systems had a much lower directional shear term than systems with linearly arranged convection, which indicates the dynamically different environments that produced these systems.

b. Severe weather reports

The inspection of the stability parameters for these systems leads directly into the discussion of severe weather. MCSs are convective, of course, by definition, so one might expect severe weather from these systems, but do certain types of systems have a propensity to produce severe weather? Table 7 provides the average number of severe weather reports for each satellite classification per MCS for tornadoes, hail, and wind as well as deaths and injuries. To be reported as severe weather, a tornado must merely be present, hail must be ¾ in. in diameter or larger, and winds must be measured at

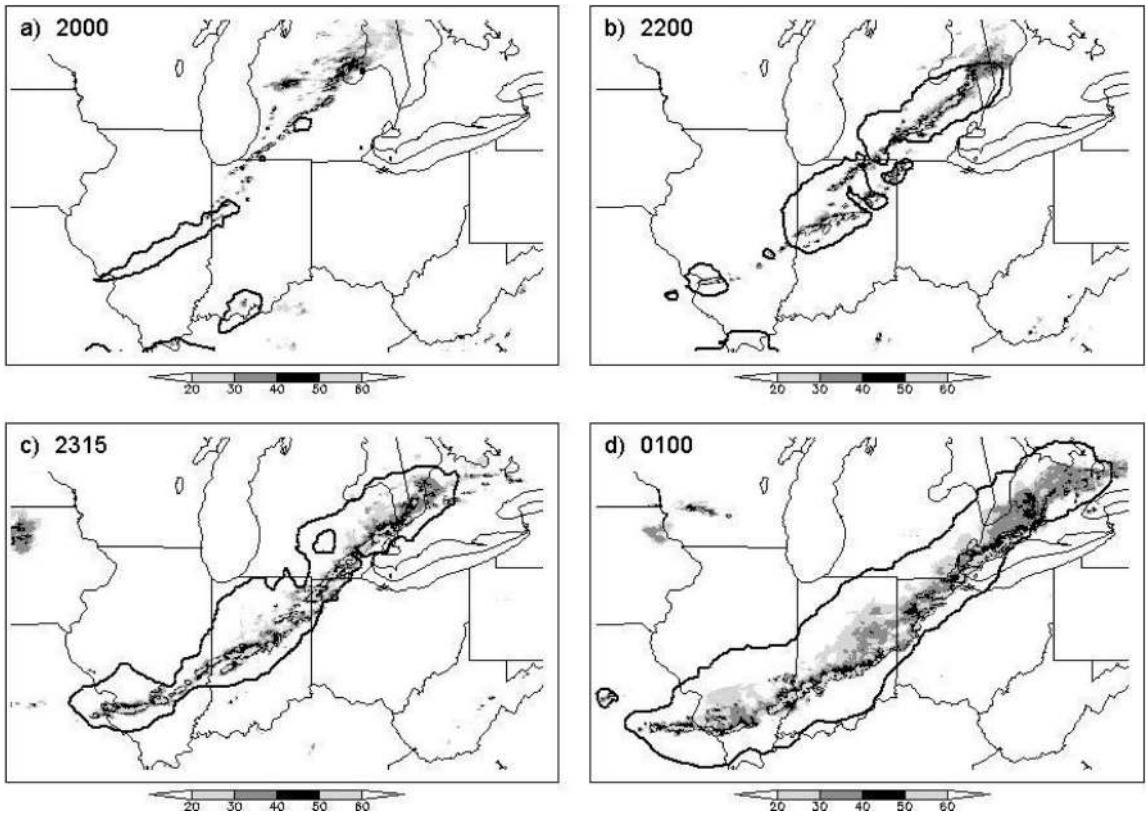

FIG. 12. Line merger development of a PECS that occurred in the upper Midwest on 21–22 Jun 1997, as seen by radar imagery. The radar reflectivity images are from: (a) 2000 UTC, (b) 2200 UTC, (c) 2315 UTC 21 Jun 1997, and (d) 0100 UTC 22 Jun 1997. The solid black contours represent the outline of the −52°C cloud shield.

greater than 50 kt at the surface. Certainly, it is important to keep in mind that population density and the number of objects that can be damaged (e.g., trees and buildings) may have an effect on the number of severe weather incidents that are reported. MCCs and PECSs accounted for most of the severe weather reports during the study period including about three tornadoes and 25 wind and hail reports per system. The smaller systems (MβCCSs and MβECSs) had many fewer severe weather reports per system with less than one tornado and about eight wind and hail reports. More than half of all severe weather reports and almost three-quarters of the reported deaths and injuries were due to PECSs even though the average severe weather indices did not show them to develop in significantly different environments from the other types of MCSs. This information reinforces the importance of PECSs as a common and violent weather system. These systems are the most severe MCS overall; however, they are not necessarily more severe per unit area than the other MCSs. When the number of severe weather reports for each system is normalized by its integrated cloud shield area throughout its life cycle, the different systems generated a similar number of severe weather reports per unit area per unit time (Fig. 17). The larger systems, though, were still more likely to produce tornadoes, as they had a nonzero median value of normalized tornado reports. Thus, the larger systems produced more severe weather reports per system primarily due to their larger size and longer duration.

In a similar fashion, the severe weather reports can be classified according to the radar developmental characteristics of each system to investigate the relationship between development and the occurrence of severe weather. Table 8 lists the average number of severe weather reports for each level of development and Fig. 18 shows the normalized severe weather reports for each category. As expected due to the environmental differences between embedded and nonembedded systems, severe weather was much more frequent with systems that were not embedded from an overall and normalized viewpoint. The areal systems also stand out as they generated significantly less severe weather than line and combination systems, which is shown by the fewer number of average and normalized severe weather reports per MCS. This agrees with the findings of Bluestein et al. (1987) that broken areal squall lines are the least likely development category to be associated with severe weather. Therefore, the arrangement of the initial convection may provide some information on the ability of the system to produce severe weather. Note that systems with linearly arranged convection (i.e., line and

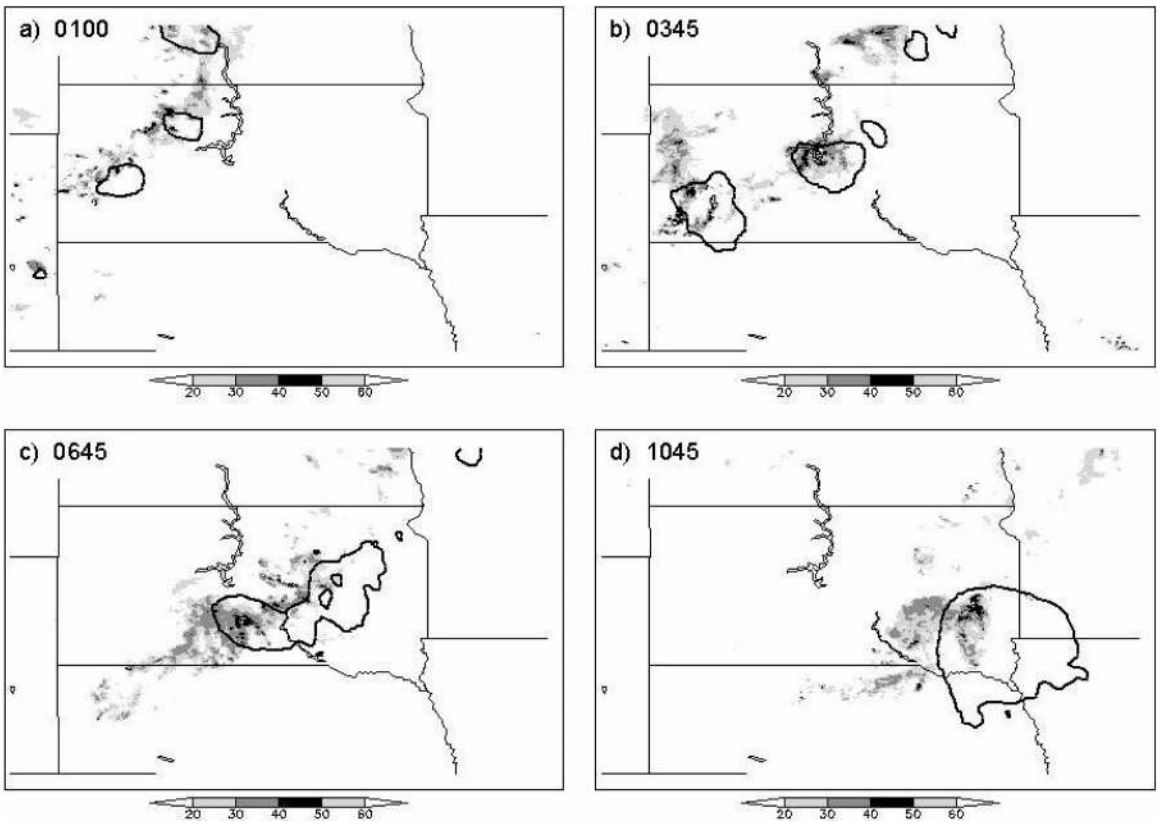

FIG. 13. Embedded areal merger development of a MβCCS that occurred in South Dakota on 25 Aug 1997, as seen by radar imagery. The radar reflectivity images are from: (a) 0100, (b) 0345, (c) 0645, and (d) 1045 UTC. The solid black contours represent the outline of the -52°C cloud shield.

combination systems) produced a high frequency of wind reports, which is consistent with the bow echo relationship to derechos (Johns and Hirt 1987). Looking at the cluster interaction categories, the merger systems tended to have more severe weather reports than nonmerger and isolated systems per system, but Fig. 18 shows that all of the cluster interaction categories produced a similar number of severe weather reports per unit area per unit time.

c. MCS satellite life cycle

The life cycles of the various MCS classifications were combined, or composited, to allow for a general overview of each category's life cycle. The systems were composited by normalizing the life cycle of each system according to the average growth stage (initiation to maximum extent) and the average dissipation stage (maximum extent to termination) for each MCS category. This normalization allows systems of all durations, growth rates, and decay rates to be composited. The areas of the $-52°$, $-58°$, $-64°$, and -70°C blackbody temperature thresholds were averaged at each normalized MCS time in order to create a composite lifecycle. Figure 19 shows the composite for the entire MCS sample. In this figure, the areas of the aforementioned IR temperature thresholds are plotted against the MCS timescale with ''00'' representing the initiation of the systems, as demarcated by a vertical line. The middle vertical line indicates the time of maximum extent of the composite; thus, the period between these first two lines represents the growth stage of the systems. The vertical line on the right signifies the termination of the systems, so the period between the second two lines represents the decay stage of the systems.

The satellite life cycles of each MCS category had very similar features with the scale being the primary difference among the life cycles. One common feature displayed in Fig. 19 and found in all of the satellite composites is that the areas of colder temperature thresholds reach a maximum before the warmer thresholds. For example, Fig. 19 shows that the area of the -58°C cloud shield peaks before the -52°C area reaches a maximum. In addition, the growth stage of MCSs generally lasts an hour longer than the decay stage.

d. MCS radar life cycle

The normalized MCS timescale developed to produce composite satellite life cycles was also used to create

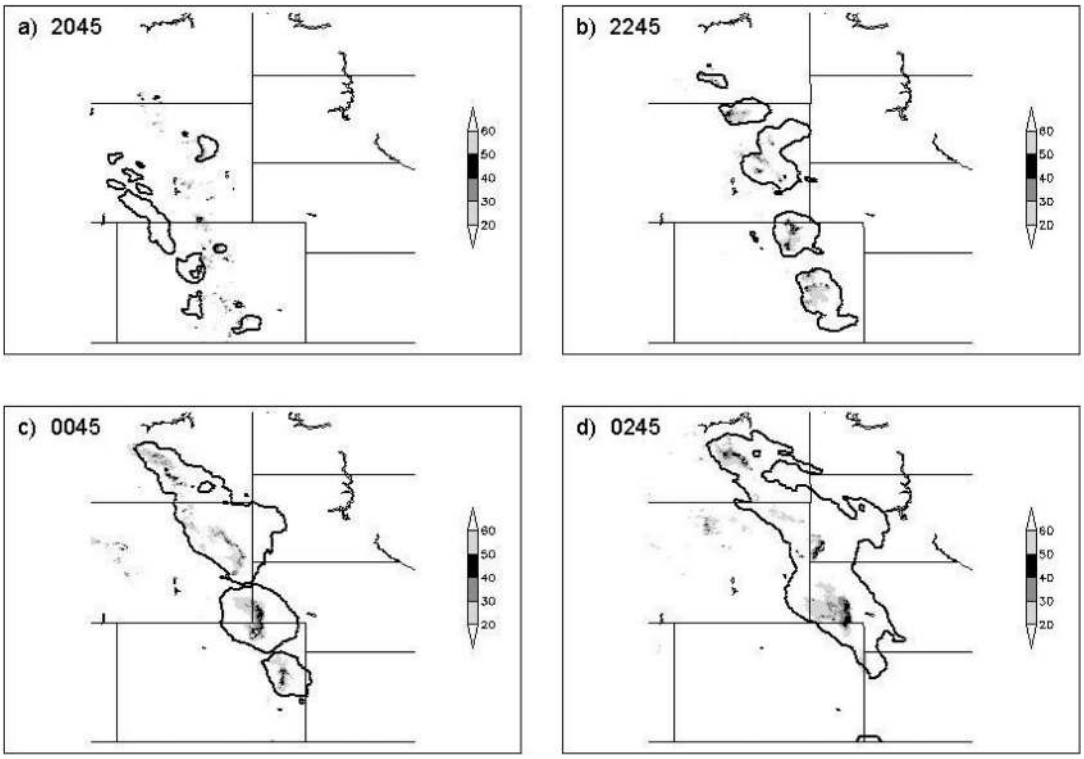

FIG. 14. Areal nonmerger development of a PECS that occurred east of the Rocky Mountains on 26–27 May 1998, as seen by radar imagery. The radar reflectivity images are from: (a) 2045 UTC, and (b) 2245 UTC 26 May 1998, (c) 0045 UTC, and (d) 0245 UTC 27 May 1998. The solid black contours represent the outline of the −52°C cloud shield.

composite radar life cycle plots. Thus, the vertical lines in Fig. 20 still represent the start, maximum, and end times of the *satellite* life cycle. There are three curves plotted in these figures: the solid curve represents system-total volumetric rain rate, V, calculated using the WSR-080 default Z–R relationship as described in section 3; the thick, dashed curve represents the precipitation area, A (defined as the reflectivity area ≥ 20 dBZ); and the thin, dashed curve represents the average rain rate, $\overline{R}$, which is calculated as $\overline{R} = V/A$.

The radar life cycle plots for each MCS category were also very much alike with similar trends and properties,

TABLE 4. Distribution of MCS radar development by satellite classification.

Development type	MCC	PECS	MβCCS	MβECS	Total
Embedded line merger	1	4	0	1	6
Embedded areal merger	6	6	7	6	25
Embedded combination merger	3	7	1	4	15
Embedded line nonmerger	0	0	0	0	0
Embedded areal nonmerger	0	0	0	1	1
Embedded combination nonmerger	0	0	0	0	0
Embedded line isolated	0	1	2	1	4
Embedded areal isolated	3	3	4	4	14
Line merger	4	20	2	5	31
Areal merger	26	34	20	25	105
Combination merger	27	41	9	16	93
Line nonmerger	0	3	0	1	4
Areal nonmerger	4	7	6	4	21
Combination nonmerger	3	3	0	0	6
Line isolated	3	7	2	6	18
Areal isolated	9	8	10	7	34
Unclassifiable	1	5	2	2	10
Total	90	149	65	83	387

TABLE 5. Distribution of MCS development by satellite classification broken into the three levels of the radar classification scheme.

Development type	MCC (90)	PECS (149)	MβCCS (65)	MβECS (83)	Total (387)
Embedded	13	21	14	17	65
Not embedded	76	123	49	64	312
Line	8	35	6	14	63
Areal	48	58	47	47	200
Combination	33	51	10	20	114
Merger	67	112	29	57	275
Nonmerger	7	13	6	6	32
Isolated	15	19	18	18	70
Unclassifiable	1	5	2	2	10

TABLE 6. Statistics for each radar development level: Means and std devs ( ).

Development type	No.	Maximum area (km²)	Duration (h)	Eccentricity
Embedded	65	130 072 (94 786)	9.3 (4.8)	0.66 (0.22)
Not embedded	312	162 581 (120 256)	9.0 (3.7)	0.64 (0.19)
Line	63	191 393 (122 282)	9.3 (3.3)	0.54 (0.19)
Areal	200	129 768 (96 761)	8.4 (3.8)	0.69 (0.18)
Combination	114	185 688 (133 784)	10.2 (4.1)	0.63 (0.19)
Merger	275	162 819 (117 531)	9.3 (3.9)	0.64 (0.19)
Nonmerger	32	184 195 (165 548)	9.0 (4.3)	0.61 (0.21)
Isolated	70	121 577 (73 629)	8.3 (3.6)	0.68 (0.18)
Unclassifiable	10	191 401 (121 890)	8.9 (5.4)	0.60 (0.18)

but different scales. The radar life cycle composite for all systems (Fig. 20) shows several common features of an average MCS life cycle for this study. One feature reveals that the average rainfall rate reaches a maximum very early in the life cycle at about the time of MCS initiation (left vertical line). At this time, the area of the system is also small, which indicates the presence of developing convective cells. As the system continues to grow, the average rainfall rate decreases signifying an increase in stratiform precipitation. Another feature shows that the volumetric rain rate peaks at nearly the same time as the −52°C cloud shield area (middle vertical line) even though the precipitation area continues to grow for approximately another hour.

Additional information about the precipitation characteristics of MCSs was extracted from these composites. These life cycle characteristics include the total precipitation mass, convective/stratiform partitioning, ratio of average precipitation area to the average cloud

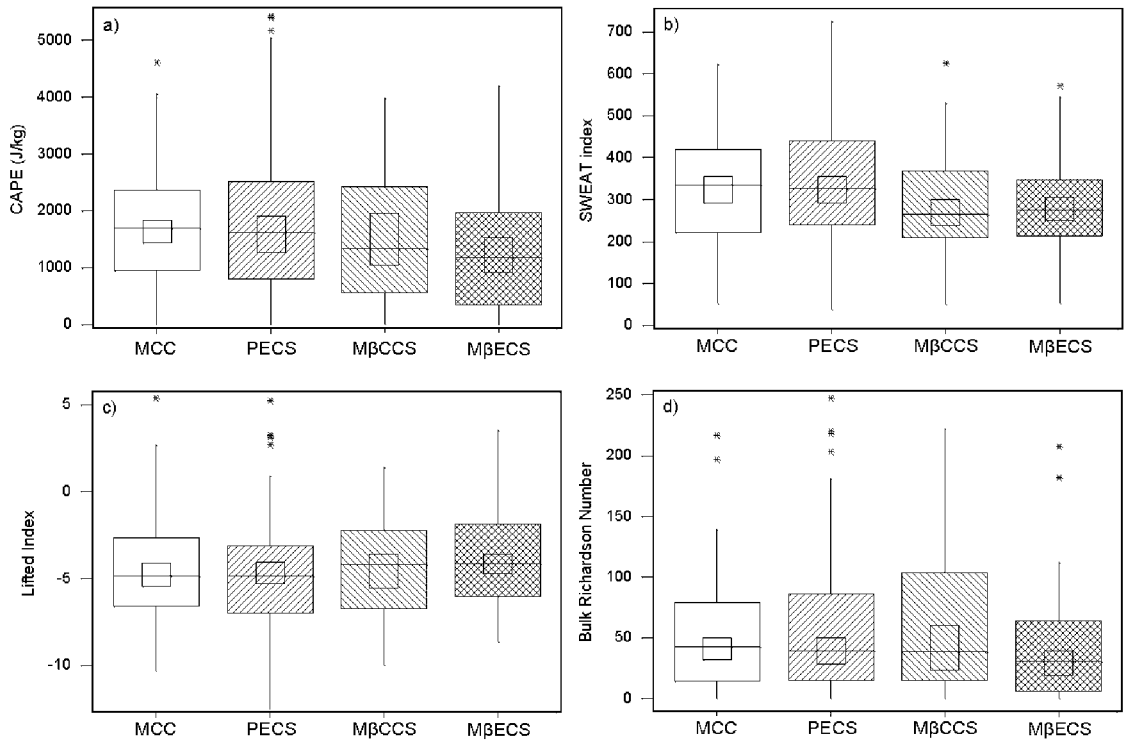

FIG. 15. Box plots for each MCS satellite classification of various sounding properties: (a) CAPE, (b) SWEAT index, (c) Lifted index, and (d) Bulk Richardson number. The wide boxes represent the interquartile range, from the 25th to the 75th percentile, and the line through this box represents the median. The ''whiskers'' extend from the box to the minimum and maximum values of the sample, or 1.5 times the interquartile range, whichever is shorter. Values outside of these limits are considered outliers and are denoted by an asterisk (*). The inner boxes show the 95% confidence interval for the median.

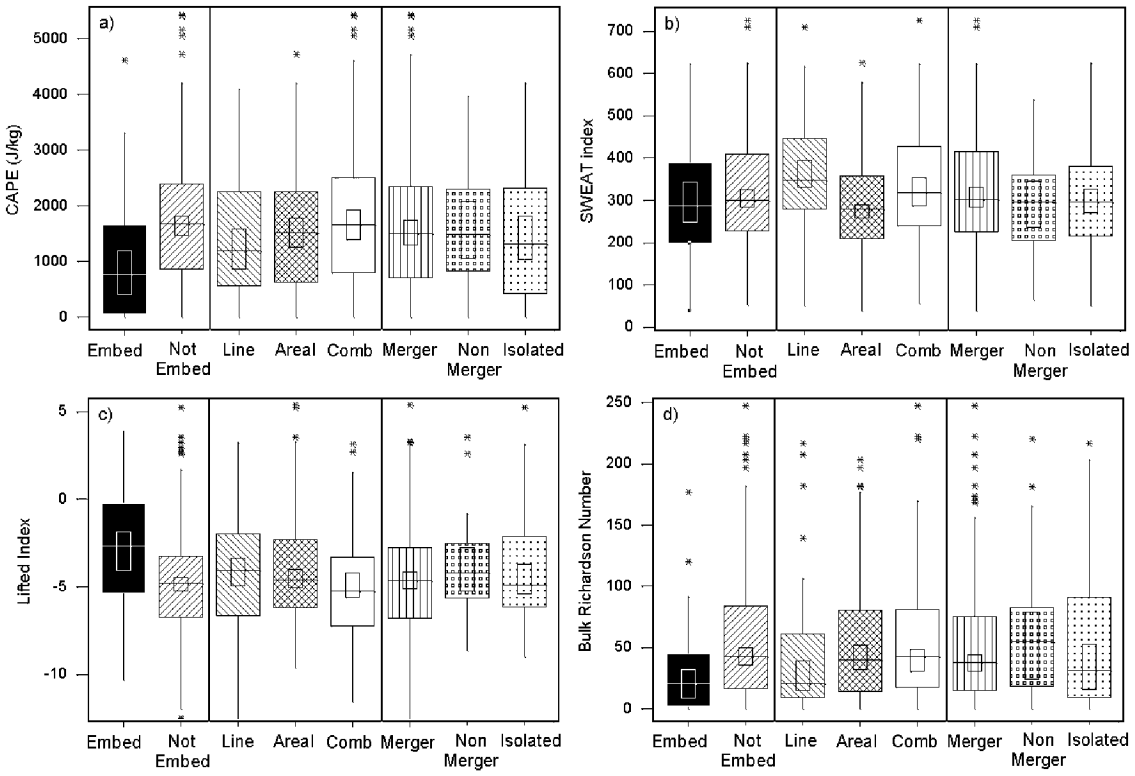

FIG. 16. Same as in Fig. 15 except for each radar development level.

shield area (at the −52°C temperature threshold), and the average depth of precipitation produced by a system over its lifetime. This theoretical precipitation depth (or normalized precipitation) corresponds to the amount of precipitation that would fall over the system's average cloud shield area provided that it remained stationary throughout its life cycle. These quantities were calculated from the composites by integrating the volumetric rain rate, precipitation area, and cloud shield area over the lifetime of the systems. The contribution to the total precipitation was divided into convective and stratiform components by choosing a convective reflectivity threshold, where everything less than the threshold was considered stratiform and everything greater than the threshold was considered convective. Steiner et al. (1995) chose 40 dB*Z* as the convective reflectivity threshold, but they also considered the gradient of the reflectivity field to include some reflectivity centers less than 40 dB*Z* as convective. Due to the large number of systems considered in this study, the reflectivity gradient was not used to determine convective precipitation; however, a range of convective reflectivity thresholds was selected in an attempt to ascertain a realistic threshold.

TABLE 7. Average number of severe weather reports per MCS for each satellite classification.

	Tornadoes	Hail	Wind	Deaths	Injuries
MCC	2.8	23.5	23.1	0.02	1.7
PECS	3.8	27.6	28.0	0.10	3.6
MβCCS	0.5	5.8	7.0	0	0.2
MβECS	0.6	9.4	9.1	0.02	0.6
All MCSs	2.3	19.1	19.3	0.04	1.9

Table 9 provides the total precipitation mass, convective percentage of precipitation, precipitation area ratio, and theoretical precipitation depth for the entire MCS sample and the satellite classifications. The total precipitation mass for the average MCC is larger than that found by McAnelly and Cotton (1989), but close to the amount for their ''large'' MCCs. This difference arises from the fact that they estimated the total precipitation mass by hourly rainfall data while the total precipitation mass for this study was estimated using radar data. The larger systems (MCCs and PECSs) were much more prolific rain-producing weather systems than the smaller systems (MβCCSs and MβECSs), generating more than 3 times as much total precipitation on average. Also, notice that at each threshold the convective contribution to precipitation was very similar for every type of MCS, regardless of the difference in total precipitation. Houze (1993) claimed that it is typical for stratiform precipitation to account for 25%–50% of the total rain in MCSs. If this is the case, then the proper convective threshold probably fell somewhere

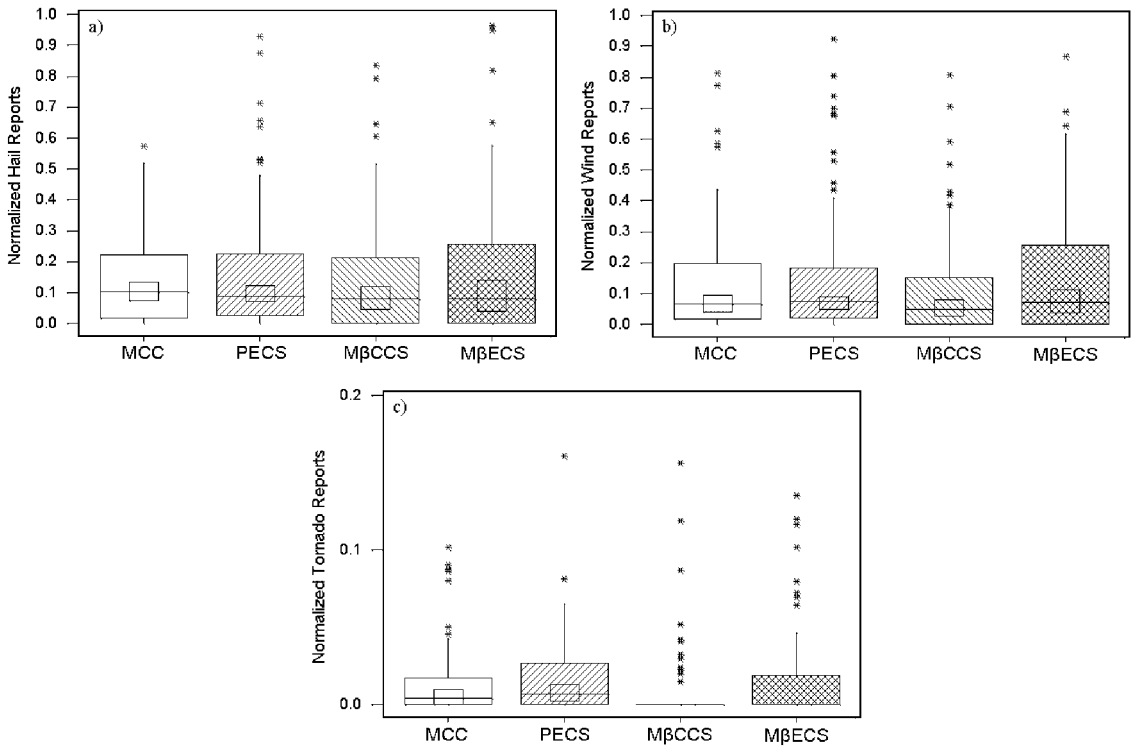

FIG. 17. Same as in Fig. 15 except for the normalized severe weather reports: (a) hail, (b) wind, and (c) tornado. The normalized values are the number of reports per 10^4 km^2 of the cold cloud shield area per hour.

between 40 and 45 dB*Z* for this MCS sample. The composite of all MCSs shows that on average almost 60% of the cold cloud shield area had underlying precipitation. MβECSs were the only type of MCS to vary significantly from that percentage, as nearly ¾ of the cloud shield produced precipitation. However, these systems still did not produce as much normalized precipitation as MCCs and PECSs. PECSs were once again the most impressive systems producing an average theoretical precipitation depth of over 5 cm.

Similarly, Table 10 shows the total precipitation mass, convective percentage, precipitation area ratio, and theoretical precipitation depth for the levels of radar development. First of all, again notice that the convective contribution to precipitation was nearly identical for all categories, except for the embedded systems. As expected from their definition, these systems had a higher percentage of stratiform precipitation as well as a high precipitation area ratio. It is also noteworthy that embedded systems and MβECSs, which formed in the most stable environments, also had the highest ratio of precipitation area to cloud shield area. Surprisingly, there was not much difference in the total precipitation and normalized precipitation between embedded systems and those that did not develop in an area of stratiform precipitation. This provides evidence that even though embedded systems may not generate a significant amount of severe weather, they are very important for the production of precipitation over the agricultural region of the central United States. Investigation of the cell arrangement categories shows that once again systems with an areal arrangement of convective cells had much different properties than systems with other types of cellular arrangement. The areal systems produced much less total precipitation and also had much smaller theoretical precipitation depths than the line and combination categories. This indicates that areal systems were relatively ineffective at producing precipitation. Finally, the interaction of convective clusters had a large

TABLE 8. Average number of severe weather reports per MCS for each radar development level.

Development type	Tornadoes	Hail	Wind	Deaths	Injuries
Embedded	1.0	11.3	12.2	0	0.6
Not embedded	2.6	20.7	20.5	0.05	3.4
Line	3.1	24.0	33.6	0.05	0.5
Areal	1.4	14.0	9.6	0.01	2.2
Combination	3.6	25.3	27.5	0.10	3.6
Merger	2.5	20.4	20.8	0.05	1.8
Nonmerger	1.8	16.6	12.9	0	0.9
Isolated	1.7	14.9	14.8	0.03	2.9
Unclassifiable	2.6	20.4	27.6	0	2.5

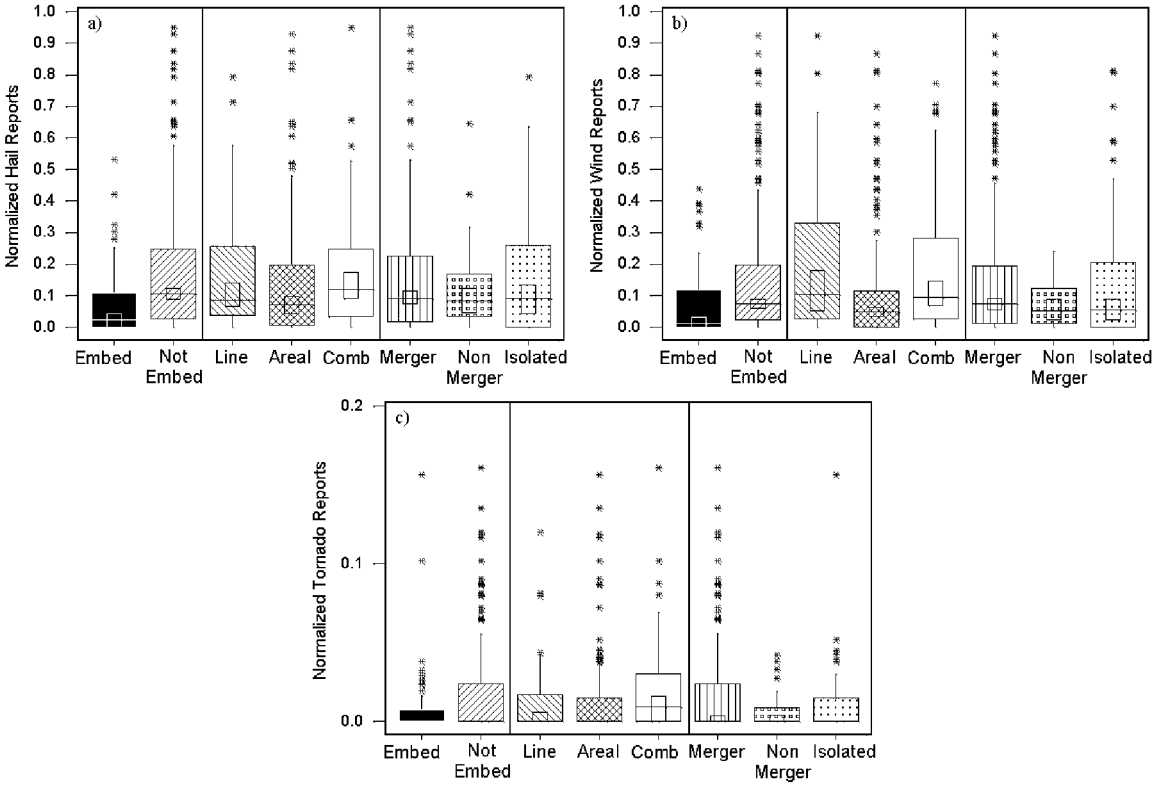

FIG. 18. Same as in Fig. 17 except for each radar development level.

influence on the ability of the MCSs to generate precipitation. Systems with merging convective clusters produced much more total and normalized precipitation than isolated or nonmerger systems. As might be expected from their definition as systems with nonmerging precipitation shields under a common cloud shield, nonmerger systems had a very low precipitation area ratio and produced less than 3 cm of rainfall on average.

7. Summary and conclusions

This study involved the identification and classification of several hundred MCSs by infrared satellite characteristics into four categories: MCCs, PECSs, MβCCSs, and MβECSs. In addition, the systems were reanalyzed with 2-km national composite radar reflectivity data to examine the developmental stages at a higher spatial and temporal resolution. The radar development of each system was categorized by a three-

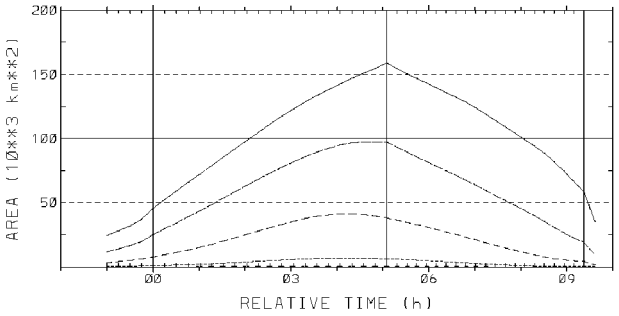

FIG. 19. Infrared satellite life cycle composite for all systems. Curves (largest to smallest magnitudes) represent the areas of the −52°, −58°, −64°, and −70°C blackbody temperature thresholds, respectively. Vertical lines represent the system initiation, maximum extent, and termination. Time is relative to system initiation.

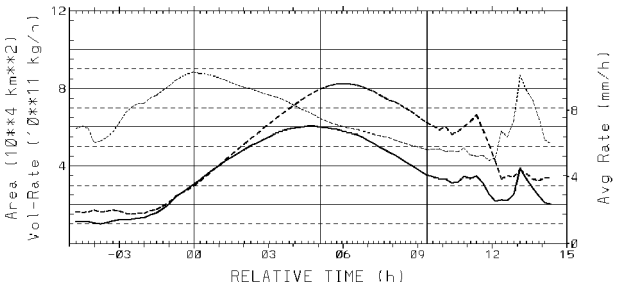

FIG. 20. Radar life cycle composite for all systems. Solid curve represents volumetric rain rate; thick, dashed curve represents precipitation area; and thin, dashed curve represents average rain rate. Vertical lines represent initiation, maximum extent, and termination of the satellite life cycle. Time is relative to system initiation.

TABLE 9. Life cycle characteristics of MCS composites for each satellite classification.

	Total precipitation mass (10^{11} kg)	Convective percentage for reflectivity thresholds of			Precipitation area ratio	Theoretical precipitation depth (cm)
		35 dB*Z*	40 dB*Z*	45 dB*Z*		
MCC	60.5	87.9	73.9	56.8	0.53	4.5
PECS	75.0	88.8	75.3	58.0	0.58	5.1
MβCCS	15.8	89.2	76.6	60.1	0.57	2.8
MβECS	23.0	88.3	75.5	58.6	0.73	3.6
All MCSs	47.0	88.5	75.1	58.0	0.59	4.2

level scheme based on the presence of stratiform precipitation, arrangement of convective cells, and interaction of convective clusters. Further analyses of each category were conducted to explore differences in the environment, severe weather reports, satellite life cycle, and precipitation life cycle among the various categories. The following findings reveal characteristics of the different MCS classifications:

- The larger satellite-defined systems, MCCs and PECSs, peaked earlier in the convective season, had larger average SWEAT indices, produced more severe weather, and generated much more precipitation than the smaller satellite-defined systems, MβCCSs and MβECSs.
- PECSs were the most dominant type of MCS as defined by satellite characteristics. They were the largest, most common, most likely to be associated with severe weather, and most proficient precipitation-producing systems.
- The radar development of more than half of the systems was by an areal merger or combination merger. Overall, less than 20% of the systems formed in the presence of stratiform precipitation, half of the systems had an areal arrangement of convective cells, and more than 70% of the systems had merging convective clusters.
- MβECSs and embedded systems developed in more stable environments than the other systems and also had the largest ratio of precipitation area to cloud shield area.
- Areal systems were statistically smaller, shorter-lived, less severe, and produced less precipitation on average than the line and combination systems.

Hopefully, the classification schemes presented in this study will prove to be flexible and practical enough for use in future MCS studies. The levels of radar development may have important implications on real-time forecasting, especially the arrangement of convective cells. Systems that originated from at least one cluster with linearly arranged convection at initiation developed into larger, longer-lived, more severe, and more proficient precipitation-producing MCSs than systems with scattered convection at initiation (i.e., areal systems), regardless of the structure of the system at maturity. This information could aid a forecaster in issuing warnings and in making short-term forecasts, as these extremely difficult and important decisions have a large impact on society.

Acknowledgments. The authors wish to thank the reviewers for their helpful comments and John Augustine for providing his MCC documentation software. The infrared satellite data and national radar composite data were provided by the Global Hydrology Resource Center. This research was supported by a National Science Foundation (NSF) Graduate Fellowship and NSF Grant ATM-9900929.

TABLE 10. Life cycle characteristics of MCS composites for each radar development level.

Development type	Total precipitation mass (10^{11} kg)	Convective percentage for reflectivity thresholds of			Precipitation area ratio	Theoretical precipitation depth (cm)
		35 dB*Z*	40 dB*Z*	45 dB*Z*		
Embedded	43.0	85.0	67.5	47.2	0.79	4.6
Not embedded	47.6	89.2	76.4	59.8	0.55	4.2
Line	67.0	89.7	76.9	59.3	0.64	5.1
Areal	32.0	87.6	73.6	56.6	0.55	3.4
Combination	65.3	88.8	75.3	58.1	0.61	5.1
Merger	51.9	88.5	74.9	57.7	0.61	4.5
Nonmerger	37.6	88.7	76.7	61.0	0.40	2.9
Isolated	32.4	88.5	76.7	61.0	0.57	3.7
Unclassifiable	52.0	89.3	77.6	62.2	0.55	4.1

APPENDIX

Sounding Indices

a. Bulk Richardson number (BRN)

$$\text{BRN} = \text{CAPE}/(0.5U^2),$$

where CAPE is the convective available potential energy ($m^2\ s^{-2}$), U is the magnitude of the shear ($u_2 - u_1$, $v_2 - v_1$), u_1, v_1 is the average u, v in the lowest 500 m, and u_2, v_2 is the average u, v in the lowest 6000 m.

b. Lifted index (LI)

$$\text{LI} = T_{e500} - T_{p500},$$

where T_{e500} is the environmental temperature in °C at 500 mb and T_{p500} is the theoretical temperature in °C a parcel of air would have at 500 mb if it were lifted dry adiabatically from the surface to its condensation level, thence moist adiabatically to 500 mb.

LI	Thunderstorm potential
>−3	Weak
−3 to −5	Moderate
<−5	Strong

*c. Total Totals (*TT*)*

$$TT = T_{850} - T_{d850} - 2 \times T_{500},$$

where T_{850} is the temperature in °C at 850 mb, T_{d850} is the dewpoint temperature in °C at 850 mb, and T_{500} is the temperature in °C at 500 mb.

TT	Thunderstorm potential
<45	Weak
45–55	Moderate
>55	Strong

d. SWEAT index (SWEAT)

$$\begin{aligned}\text{SWEAT} = {} & (12 \times T_{d850}) + [20 \times (\text{TT} - 49)] \\ & + (2 \times W_{850}) + W_{500} \\ & + \{125 \times [\sin(D_{500} - D_{850}) + 0.2]\},\end{aligned}$$

where T_{d850} is the dewpoint temperature in °C at 850 mb, TT is the Total Totals index and (TT − 49) is set to zero if negative, W_{850} is the wind speed at 850 mb in knots, W_{500} is the wind speed at 500 mb in knots, D_{850} is the wind direction at 850 mb, and D_{500} is the wind direction at 500 mb.

SWEAT	Thunderstorm potential
<300	Weak
300–399	Moderate
400–599	Strong
>600	High

REFERENCES

Air Weather Service, 1979: The use of the skew T, log p diagram in analysis and forecasting. Tech. Rep. AWS/TR-79/006, revised, 157 pp. [Available from U.S. Air Force Air Weather Service, Scott Air Force Base, IL 62225-5008.]

Anderson, C. J., and R. W. Arritt, 1998: Mesoscale convective complexes and persistent elongated convective systems over the United States during 1992 and 1993. *Mon. Wea. Rev.,* **126,** 578–599.

Augustine, J. A., 1985: An automated method for the documentation of cloud-top characteristics of mesoscale convective systems. NOAA Tech. Memo. ERL ESG-10, Dept. of Commerce, Boulder, CO, 121 pp.

——, and K. W. Howard, 1988: Mesoscale convective complexes over the United States during 1985. *Mon. Wea. Rev.,* **116,** 685–701.

Blanchard, D. O., 1990: Mesoscale convective patterns of the southern High Plains. *Bull. Amer. Meteor. Soc.,* **71,** 994–1005.

Bluestein, H. B., and C. R. Parks, 1983: A synoptic and photographic climatology of low-precipitation severe thunderstorms in the southern Plains. *Mon. Wea. Rev.,* **111,** 2034–2046.

——, and M. H. Jain, 1985: Formation of mesoscale lines of precipitation: Severe squall lines in Oklahoma during the spring. *J. Atmos. Sci.,* **42,** 1711–1732.

——, G. T. Marx, and M. H. Jain, 1987: Formation of mesoscale lines of precipitation: Nonsevere squall lines in Oklahoma during the spring. *Mon. Wea. Rev.,* **115,** 2719–2727.

Brooks, R. H., C. A. Doswell, and J. Cooper, 1994: On the environments of tornadic and nontornadic mesocyclones. *Wea. Forecasting,* **9,** 606–618.

Cotton, W. R., M. S. Lin, R. L. McAnelly, and C. J. Tremback, 1989: A composite model of mesoscale convective complexes. *Mon. Wea. Rev.,* **117,** 765–783.

——, G. D. Alexander, R. Hertenstein, R. L. Walko, R. L. McAnelly, and M. Nicholls, 1995: Cloud venting—A review and some new global annual estimates. *Earth-Sci. Rev.,* **39,** 169–206.

Fritsch, J. M., R. J. Kane, and C. R. Chelius, 1986: The contribution of mesoscale convective weather systems to the warm-season precipitation in the United States. *J. Climate Appl. Meteor.,* **25,** 1333–1345.

Fulton, R. A., J. P. Breidenbach, D.-J. Seo, D. A. Miller, and T. O'Bannon, 1998: The WSR-88D rainfall algorithm. *Wea. Forecasting,* **13,** 377–395.

Geerts, B., 1998: Mesoscale convective systems in the southeast United States during 1994–95: A survey. *Wea. Forecasting,* **13,** 860–869.

Hilgendorf, E. R., and R. H. Johnson, 1998: A study of the evolution of mesoscale convective systems using WSR-88D data. *Wea. Forecasting,* **13,** 437–452.

Houze, R. A., Jr., 1993: *Cloud Dynamics.* Academic Press, 573 pp.

——, B. F. Smull, and P. Dodge, 1990: Mesoscale organization of springtime rainstorms in Oklahoma. *Mon. Wea. Rev.,* **118,** 613–654.

Johns, R. H., and W. D. Hirt, 1987: Derechos: Widespread convectively induced windstorms. *Wea. Forecasting,* **2,** 32–49.

Loehrer, S. M., and R. H. Johnson, 1995: Surface pressure and precipitation life cycle characteristics of PRE-STORM mesoscale convective complexes. *Mon. Wea. Rev.,* **123,** 600–621.

Maddox, R. A., 1980: Mesoscale convective complexes. *Bull. Amer. Meteor. Soc.,* **61,** 1374–1387.

——, 1983: Large-scale meteorological conditions associated with

midlatitude, mesoscale convective complexes. *Mon. Wea. Rev.*, **111,** 126–140.

——, D. M. Rogers, and K. W. Howard, 1982: Mesoscale convective complexes over the United States during 1981—An annual summary. *Mon. Wea. Rev.,* **110,** 1501–1514.

McAnelly, R. L., and W. R. Cotton, 1986: Meso-β scale characteristics of an episode of meso-α scale convective complexes. *Mon. Wea. Rev.*, **114,** 1740–1770.

——, and ——, 1989: The precipitation life cycle of mesoscale convective complexes over the central United States. *Mon. Wea. Rev.*, **117,** 784–808.

Orlanski, I., 1975: A rational subdivision of scales for atmospheric processes. *Bull. Amer. Meteor. Soc.*, **56,** 527–530.

Parker, M. D., and R. H. Johnson, 2000: Organizational modes of midlatitude mesoscale convective systems. *Mon. Wea. Rev.*, **128,** 3413–3436.

Steiner, M., R. A. Houze Jr., and S. E. Yuter, 1995: Climatological characterization of three-dimensional storm structure from operational radar and rain gauge data. *J. Appl. Meteor.*, **34,** 1978–2007.

Woodley, W. L., A. R. Olsen, A. Herndon, and V. Wiggert, 1975: Comparison of gage and radar methods of convective rain measurement. *J. Appl. Meteor.*, **14,** 909–928.